Scientific Research Publishing

International Journal of Astronomy and Astrophysics, 2022, 12, 363-381
https://www.scirp.org/journal/ijaa
ISSN Online: 2161-4725
ISSN Print: 2161-4717

Measurement of the Dark Matter Velocity Dispersion with Dwarf Galaxy Rotation Curves

Bruce Hoeneisen

Universidad San Francisco de Quito, Quito, Ecuador
Email: bhoeneisen@usfq.edu.ec

How to cite this paper: Hoeneisen, B. (2022) Measurement of the Dark Matter Velocity Dispersion with Dwarf Galaxy Rotation Curves. *International Journal of Astronomy and Astrophysics*, **12**, 363-381.
https://doi.org/10.4236/ijaa.2022.124021

Received: September 20, 2022
Accepted: December 26, 2022
Published: December 29, 2022

Abstract

Warm dark matter has, by definition, a velocity dispersion. Let $v_{hrms}(a) = v_{hrms}(1)/a$ be the root-mean-square velocity of non-relativistic warm dark matter particles in the early universe at expansion parameter a. $v_{hrms}(1)$ is an adiabatic invariant. We obtain $v_{hrms}(1)$ in the core of 11 dwarf galaxies dominated by dark matter, from their observed rotation curves, up to a rotation and relaxation correction. We obtain a mean 0.490 km/s and standard deviation 0.160 km/s, with a distribution peaked at the lower end. We apply a mild, data driven, rotation and relaxation correction that obtains the adiabatic invariant in the core of the galaxies: $v_{hrms}(1) = 0.406 \pm 0.069$ km/s. These two small relative standard deviations justify the prediction that the adiabatic invariant $v_{hrms}(1)$ in the core of the galaxies is of cosmological origin if dark matter is warm. This result is in agreement with measurements of $v_{hrms}(1)$ based on spiral galaxy rotation curves, galaxy ultra-violet luminosity distributions, galaxy stellar mass distributions, the formation of first galaxies, reionization, and the velocity dispersion cut-off mass.

Keywords

Warm Dark Matter, Galaxy Rotation Curves, Dwarf Galaxies

1. Introduction

We consider non-relativistic dark matter as a classical (non-degenerate) gas, with negative chemical potential, as justified in [1] [2]. Let $v_{hrms}(a)$ be the root-mean-square velocity of non-relativistic dark matter particles in the early universe at expansion parameter a (normalized to $a = 1$ at the present time). As the universe expands it cools, so $v_{hrms}(a)$ is proportional to a^{-1} (if dark matter collisions, if any, do not excite particle internal degrees of freedom, see di-

gression below). Therefore

$$v_{h\mathrm{rms}}(1) = v_{h\mathrm{rms}}(a)\,a = v_{h\mathrm{rms}}(a)\left[\frac{\Omega_c \rho_{\mathrm{crit}}}{\rho_h(a)}\right]^{1/3}, \tag{1}$$

is an adiabatic invariant. $\rho_h(a) \propto a^{-3}$ is the density of dark matter, and $\Omega_c \rho_{\mathrm{crit}} \equiv \rho_h(1)$. (We use the standard notation in cosmology, and the parameters, as in [3]. Throughout, the subscript h refers to dark matter, and the subscript b will refer to baryons, *i.e.* gas and stars.) The purpose of this study is to obtain $v_{h\mathrm{rms}}(1)$ from the rotation curves of dwarf galaxies dominated by a dark matter halo, and with a thin disk of rotating gas and stars (that allows the measurement of the galaxy rotation curves). If the measured $v_{h\mathrm{rms}}(1)$ turns out to be consistent with zero, we say that dark matter is cold. If $v_{h\mathrm{rms}}(1)$ turns out to be significantly greater than zero, we say that dark matter is warm (if already non-relativistic when densities of radiation and matter are equal).

Our prediction, which needs confirmation by data, is this. Consider a free observer in the center of a spherically symmetric density perturbation in the early universe. This observer feels no gravity, and "sees" dark matter expand adiabatically, reach turn-around, and contract adiabatically into the core of a galaxy (note that if dark matter is warm the galaxy forms a core adiabatically [4]). Since $v_{h\mathrm{rms}}(1)$ is an adiabatic invariant, we predict that $v_{h\mathrm{rms}}(1)$ has the same value in the core of all relaxed galaxies, and is of cosmological origin. There are two subtleties to this argument. One is that what we are able to measure is $v'_{h\mathrm{rms}}(1) \equiv v_{h\mathrm{rms}}(1)/\sqrt{1-\kappa_h}$, where $\sqrt{1-\kappa_h}$ is a dark matter rotation correction factor, with $0 \le \kappa_h < 1$. $\kappa_h = 0$ if the dark matter particle orbits are radial, while $\kappa_h \to 1$ if the dark matter particles approach circular orbits. κ_h is largely unknown. The second issue is "phase space dilution" due to non-adiabatic processes, e.g. galaxy interactions and mergers with relaxation, or the formation of galaxies with relaxation and "virialization" in the cold dark matter scenario. To obtain $v_{h\mathrm{rms}}(1)$, we will have to deal with these two issues.

Digression: Due to the subtleties of self-gravitating dark matter, it is convenient to recall how (1) can be derived for non-relativistic particles. 1) Consider an expanding universe. The velocity of a free particle with respect to that comoving observer that is momentarily at the position of the particle, is proportional to a^{-1}. To obtain this result use Hubble's law with $H = a^{-1}\mathrm{d}a/\mathrm{d}t$. 2) The adiabatic expansion of a collisional, or collisionless, classical noble gas satisfies $T/\rho^{\gamma-1} = \text{constant}$, with $\gamma = 5/3$. Since $T \propto \langle v^2 \rangle$, and $\rho \propto a^{-3}$, $\langle v^2 \rangle \propto a^{-2}$. 3) To define "orbitals", *i.e.* volumes in phase space, apply periodic boundary conditions to an expanding box. The momentum of each orbital satisfies $p(a) = h/\lambda \propto a^{-1}$ (valid for ultra-relativistic or non-relativistic particles). So $p_{h\mathrm{rms}}(a)\,a$ is constant if the mean numbers of particles per orbital remain constant. 4) To prove that a free particle has momentum $\boldsymbol{p} \propto a^{-1}$ use the argument in 1) with a Lorentz transformation. 5) The Collisionless Boltzmann Equation expresses that the number of particles per unit phase-space volume, as seen by any free particle, is constant (in the approximation of being colli-

sionless and conserved), which again leads to $p_{hrms}(a) \propto a^{-1}$. 6) The relation $v_{hrms}(a)a = \text{constant}$ can also be obtained from the ideal noble gas Sackur-Tetrode entropy = constant.

We have already carried out this measurement with 46 spiral galaxies in the "Spitzer Photometry and Accurate Rotation Curves" (SPARC) sample, obtaining a distribution of $v'_{hrms}(1)$ with mean 0.915 km/s, and standard deviation 0.332 km/s [5], see **Figure 1**. This small relative standard deviation is noteworthy, and, considering that the galaxies span three orders of magnitude in luminosity, and considering the uncertainties from rotation and relaxation, gives support to the argument above. The hope with the present analysis with dwarf galaxies dominated by dark matter, is to obtain the distribution of $v'_{hrms}(1)$ with different systematic uncertainties, to better constrain the corrections for the unknown κ_h and the stellar mass-to-luminosity ratio Υ_*, and to more reliably extract the adiabatic invariant $v_{hrms}(1)$.

In section 2 we discuss the hydrostatic equations that describe two self-gravitating gases, dark matter and baryons, and their solutions. In section 3 we obtain $v'_{hrms}(1)$ from the rotation curves measured by Se-Heon Oh *et al.* [6], based on the "Local Irregulars That Trace Luminosity Extremes—The HI Nearby Galaxy Survey" (LITTLE THINGS), and additional infrared and visible images. Systematic uncertainties are discussed in section 4, the final adiabatic invariant is obtained in section 5, followed by comments, a discussion on relaxation, and conclusions. Measured and calculated rotation curves are collected in the appendix.

2. Hydrostatic Equations

The hydrostatic equations that describe two self-gravitating gases (dark matter

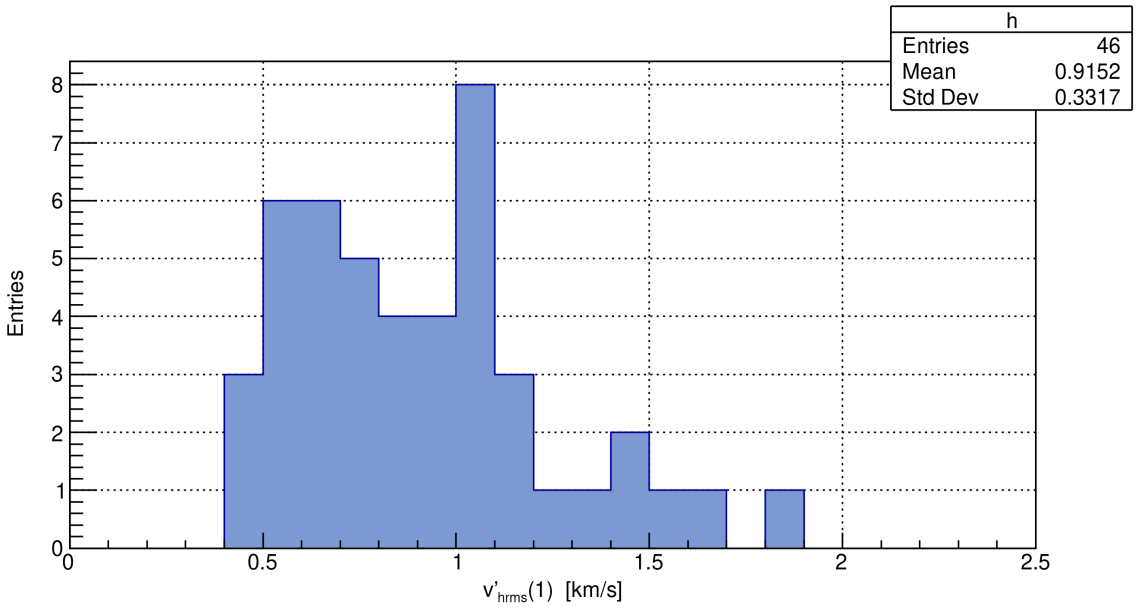

Figure 1. Distribution of $v'_{hrms}(1) \equiv v_{hrms}(1)/\sqrt{1-\kappa_h}$, *i.e.* the adiabatic invariant before the dark matter rotation correction, of 46 spiral galaxies in the SPARC sample [5].

and baryons) are Newton's equation, and the time-independent limit of the radial component of Jeans Equation, (a moment of the Collisionless Boltzmann Equation, or $\boldsymbol{F} = \mathrm{d}\boldsymbol{p}/\mathrm{d}t$ in disguise): [4] [7] [8]

$$\nabla \cdot \boldsymbol{g} = -4\pi G\left(\rho_h + \rho_b\right), \tag{2}$$

$$\left(1-\kappa_h\right)\rho_h \boldsymbol{g} = \nabla\left(\left\langle v_{rh}^2\right\rangle \rho_h\right), \tag{3}$$

$$\left(1-\kappa_b\right)\rho_b \boldsymbol{g} = \nabla\left(\left\langle v_{rb}^2\right\rangle \rho_b\right). \tag{4}$$

We have included the parameters κ_h and κ_b to describe dark matter and baryon rotation, respectively. $\kappa_h \equiv v_h^2(r)/v^2(r)$ and $\kappa_b \equiv v_b^2(r)/v^2(r)$, where $v(r) = \sqrt{|g(r)|r}$ is the velocity of a test particle in a circular orbit of radius r in the plane of the baryon disk, and $v_h(r)$ and $v_b(r)$ are the contributions, from dark matter and baryons, to $v(r) = \sqrt{v_h^2(r) + v_b^2(r)}$. ($\sqrt{\kappa_h}$ is approximately equal to the galaxy "spin parameter" of P.J.E. Peebles: $\lambda \equiv J|E|^{1/2}/\left(GM^{5/2}\right)$, where $J \approx MRv_h$ is angular momentum, and $E \approx -GM^2/R$ is energy). Equations (3) and (4) can also be understood as momentum conservation equations, separately for particles with $v_{rh} > 0$ and $v_{rh} < 0$. These equations are approximate for the problem at hand. (We could have considered separate equations for stars and gas. The equation for gas is the Euler Equation, *i.e.* $\sqrt{\left\langle v_r^2\right\rangle}$ is replaced by the sound velocity). For a full discussion, see [9].

We make the data driven approximations that κ_h, κ_b, $\left\langle v_{rh}^2\right\rangle$ and $\left\langle v_{rb}^2\right\rangle$ are independent of r, since, with these approximations, we obtain excellent fits to the galaxy rotation curves, see the appendix, and references [5] and [8]. These approximations can be understood as follows. The (arguable) independence of $\left\langle v_{rh}^2\right\rangle$ and $\left\langle v_{rb}^2\right\rangle$ on r corresponds to thermal equilibrium, *i.e.* to the non-relativistic Boltzmann distribution, separately for dark matter and baryons, and is non-trivial, see the beautiful discussions in the chapter "The exponential atmosphere" in "The Feynman Lectures on Physics" to appreciate the subtleties of thermal equilibrium, and to understand the right-hand-side of Equations (3) and (4). In the warm dark matter scenario, the radius of the halo grows with velocity $\sqrt{3\left\langle v_{rh}'^2\right\rangle}$, and the particles becoming bound by gravity populate the tail of the non-relativistic isothermal Boltzmann distribution [10]. Note that if $\rho_h(r) \gg \rho_b(r)$ at large r, $\left\langle v_{rh}'^2\right\rangle$ independent of r results in the observed flat rotation velocity $v(r) = V_{\text{flat}}$ at large r. As we shall see, $\kappa_b \approx 0.99$, while κ_h is largely unknown.

Note that (3) depends on $\left\langle v_{rh}'^2\right\rangle \equiv \left\langle v_{rh}^2\right\rangle/\left(1-\kappa_h\right)$, and (4) depends on $\left\langle v_{rb}'^2\right\rangle \equiv \left\langle v_{rb}^2\right\rangle/\left(1-\kappa_b\right)$, so, to measure $\left\langle v_{rh}^2\right\rangle$ from rotation curves, it is necessary to obtain κ_h from an independent source.

We consider the case $\rho_h(r) \gg \rho_b(r)$ that corresponds to the dwarf galaxies in the present study, and assume spherical symmetry. There is a 2-parameter family of solutions, defined by the core density $\rho_c \equiv \rho_h(r \to 0)$ and $\left\langle v_{rh}'^2\right\rangle$. Given these boundary conditions, the solution has a core radius r_c, and an asymptotic density, given by

$$r_c = \sqrt{\frac{\langle v'^2_{rh} \rangle}{2\pi G \rho_c}}, \quad \rho_h(r) = \frac{\langle v'^2_{rh} \rangle}{2\pi G r^2} \quad \text{for } r \gg r_c. \tag{5}$$

The adiabatic invariant (1) in the core of the galaxy is

$$v_{hrms}(1) = \sqrt{3}\sqrt{\langle v^2_{rh} \rangle}\left[\frac{\Omega_c \rho_{crit}}{\rho_c}\right]^{1/3}. \tag{6}$$

The results in (5) can be approximated by the "pseudo-isothermal sphere"

$$\rho_h(r) = \frac{\rho_c}{1+(r/r_c)^2} \tag{7}$$

(the exact solution is given in [9] [11]) corresponding to the circular velocity

$$\begin{aligned} v_h(r) &= \sqrt{4\pi G \rho_c r_c^2 \left[1 - \frac{r_c}{r}\arctan\left(\frac{r}{r_c}\right)\right]} \\ &= \begin{cases} \sqrt{4\pi G \rho_c} r_c \equiv V_{flat} = \sqrt{2}\sqrt{\langle v'^2_{rh} \rangle} & \text{for } r \to \infty, \\ \sqrt{\frac{4}{3}\pi G \rho_c} r & \text{for } r \to 0. \end{cases} \end{aligned} \tag{8}$$

Note that the circular velocity at large r obtains $\sqrt{\langle v'^2_{rh} \rangle}$, while the slope of the circular velocity at small r obtains ρ_c. These two parameters obtain $v'_{hrms}(1) \equiv v_{hrms}(1)/\sqrt{1-\kappa_h}$, *i.e.* the adiabatic invariant uncorrected for dark matter rotation.

The solution for baryons at large r is $\rho_b(r) \propto r^{-2\alpha}$ with $\alpha \equiv \langle v'^2_{rh} \rangle / \langle v'^2_{rb} \rangle$. At the time of the galaxy formation, $\alpha \approx 1$ [4]. As baryons loose energy by radiation, α increases, and baryons become localized, *i.e.* their mass within large r eventually converges, when $2\alpha > 3$.

3. Data Analysis

The data source of the present study is obtained from the Se-Heon Oh *et al.* state-of-the art analysis in [6], based on the LITTLE THINGS survey [12], combined with *Spitzer* 3.6 μm images [13], and additional *U*, *B*, and *V* optical images [14], to obtain mass models of 26 late-type dwarf galaxies. The LITTLE THINGS survey collects data with the very large radio interferometer array Karl G. Jansky VLA[1] that observes the 21 cm hyperfine line of atomic hydrogen (HI) of nearby dwarf galaxies (at distances less than 11 Mpc, with ≈ 6" angular resolution, and <2.6 km/s velocity resolution [12]).

From the 26 dwarf galaxies studied in [6], we select those that satisfy these criteria: 1) $v_h(r) > v_b(r)$ to obtain a reliable dark matter rotation curve; 2) $v(r)$ reaches V_{flat} so $\sqrt{\langle v'^2_{rh} \rangle}$ is well measured; and 3) $v(r)$ has a rising segment at small r so ρ_c is well measured. Finally, we remove the blue compact dwarf galaxy Haro 29 that is extremely irregular [6] (see the rotation curve

[1]The VLA is a facility of the National Radio Astronomy Observatory (NRAO). The NRAO is a facility of the National Science Foundation operated under cooperative agreement by Associated Universities, Inc.

at the end of the appendix), indicating a probable recent interaction [15]. This selection leaves the 11 galaxies listed in **Table 1**, at distances between 3 Mpc and 11 Mpc, except WLM at 1 Mpc, *i.e.* outside of the Milky Way.

The Se-Heon Oh *et al.* collaboration [6] obtains the galaxy rotation curves, subtracts the baryon (gas and stellar) contribution, fits the resulting dark matter rotation curves to the pseudo-isothermal template (8), and obtains ρ_c and r_c. From ρ_c and r_c, we obtain the adiabatic invariant $v_{h\mathrm{rms}}(1)$ of warm dark matter, uncorrected for dark matter rotation, as follows:

$$v'_{h\mathrm{rms}}(1) \equiv \frac{v_{h\mathrm{rms}}(1)}{\sqrt{1-\kappa_h}} = \sqrt{3}\sqrt{\langle v'^2_{rh}\rangle}\, a = \sqrt{\frac{3}{2}V^2_{\mathrm{flat}}}\, a = \sqrt{6\pi G\rho_c r_c^2}\left(\frac{\Omega_c \rho_{\mathrm{crit}}}{\rho_c}\right)^{1/3}. \quad (9)$$

Note that a knowledge of κ_h, independently of the rotation curves, is needed to apply the correction factor $\sqrt{1-\kappa_h}$, to finally obtain the adiabatic invariant $v_{h\mathrm{rms}}(1)$. The results are summarized in **Table 1** and **Figure 2**. The mean and standard deviation of $v'_{h\mathrm{rms}}(1)$ are 0.568 km/s and 0.208 km/s, respectively.

As an alternative analysis, we integrate numerically Equations (2)-(4) in spherical coordinates, starting from the first measured point at $r_{\min}$, and ending at the last measured point at $r_{\max}$. To start these integrations it is necessary to provide four boundary conditions: $\sqrt{\langle v'^2_{rb}\rangle}$, $\sqrt{\langle v'^2_{rh}\rangle}$, $\rho_b(r_{\min})$, and $\rho_h(r_{\min})$. These four parameters are varied to minimize a χ^2 between the measured and calculated rotation curves. The uncertainties of $v(r)$ are provided in [6]. To define the χ^2 it is necessary to assign uncertainties to the baryon contribution. We do this by eye, guided by the fluctuations in the baryon contribution (that is sub-dominant). The data is compared with the numerical integrations in the

Table 1. Presented are 11 dwarf galaxies passing the selections (see text), their central dark matter density ρ_c, and core radius r_c, from [6], and the calculated $v'_{h\mathrm{rms}}(1)$ from (9). Uncertainties are statistical from [6]. The mean and standard deviation of $v'_{h\mathrm{rms}}(1)$ are 0.568 km/s and 0.208 km/s, respectively.

Galaxy	ρ_c [$10^{-3} M_\odot/\mathrm{pc}^3$]	r_c [kpc]	$v'_{h\mathrm{rms}}(1)$ [km/s]
DDO 43	33.22 ± 8.78	0.94 ± 0.18	0.488 ± 0.115
DDO 46	517.82 ± 65.46	0.51 ± 0.04	0.419 ± 0.042
DDO 52	48.81 ± 3.63	1.33 ± 0.07	0.737 ± 0.048
DDO 87	13.91 ± 0.77	2.46 ± 0.11	1.105 ± 0.060
DDO 101	849.14 ± 77.23	0.32 ± 0.01	0.285 ± 0.013
DDO 126	21.59 ± 2.00	1.33 ± 0.10	0.643 ± 0.058
DDO 133	73.69 ± 7.61	0.83 ± 0.06	0.492 ± 0.044
DDO 154	53.21 ± 3.19	0.95 ± 0.03	0.534 ± 0.022
NGC 2366	43.89 ± 2.51	1.21 ± 0.04	0.658 ± 0.028
NGC 3738	2132.36 ± 277.75	0.45 ± 0.04	0.468 ± 0.052
WLM	57.46 ± 1.57	0.74 ± 0.01	0.421 ± 0.008

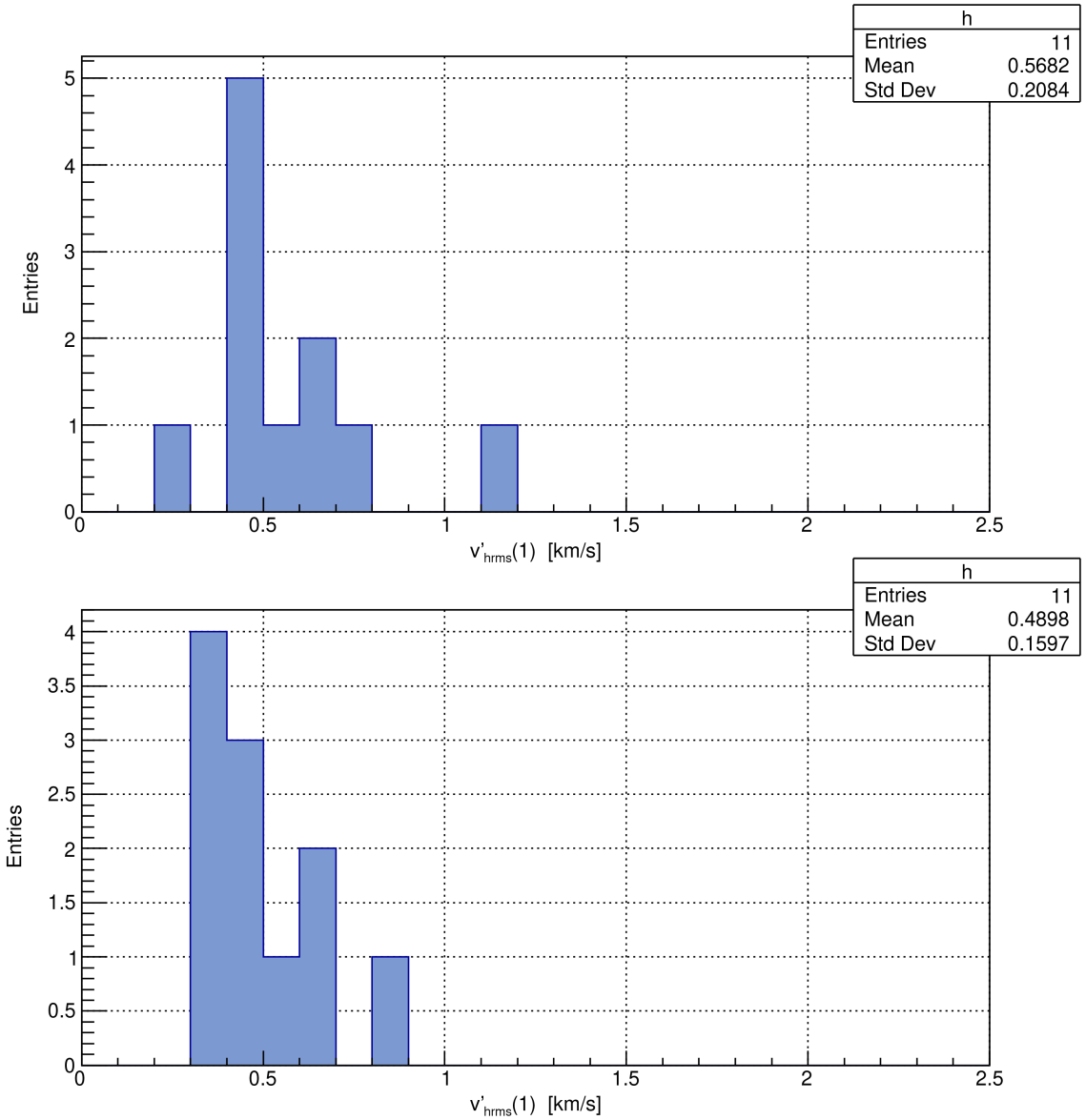

Figure 2. Distribution of $v'_{hrms}(1) \equiv v_{hrms}(1)/\sqrt{1-\kappa_h}$, *i.e.* the adiabatic invariant before the dark matter rotation correction, of 11 dwarf galaxies from Table 1 (upper panel), and Table 2 (lower panel).

appendix. The results are summarized in Table 2 and Figure 2. The mean and standard deviation of $v'_{hrms}(1)$ are 0.490 km/s and 0.160 km/s, respectively. Note that $\sqrt{\langle v'^2_{rh}\rangle}$ depends mainly on the data points of $v(r)$ at large r, while $\rho_h(r_{\min})$ depends mainly on the data points at small r.

The two distributions in Figure 2, corresponding to Table 1 and Table 2, are different. The difference has contributions from the different assumptions of these two analyses. Table 1 assumes the "pseudo-isothermal sphere", *i.e.* fits to the template (8), while Table 2 assumes dark matter is exactly isothermal, *i.e.* $\sqrt{\langle v'^2_{rh}\rangle}$ = constant. The difference between these two assumptions is non-negligible, and is studied in detail in [11]. In the present article we favor $\sqrt{\langle v'^2_{rh}\rangle}$ = constant because it corresponds to dark matter particles with the non-relativistic isother-

mal Boltzmann distribution that is justified in [1].

We choose Table 2 as our final result for the adiabatic invariant before correcting for rotation (which is also the method used in [5]). The distributions in Table 2 and in the SPARC sample [5] are compared in Figure 3.

4. Systematic Uncertainties

If dark matter is cold, the distributions in Figures 1-3 are the result of galaxy formation, relaxation and "virialization". In this case, what sets the scale of $v'_{hrms}(1)$, and why is its distribution so narrow relative to the mean? We consider the alternative, that dark matter is warm, and $v_{hrms}(1)$ is an adiabatic invariant of cosmological origin. If dark matter is warm, what phenomenon sets the width of $v'_{hrms}(1) \equiv v_{hrms}(1)/\sqrt{1-\kappa_h}$?

We consider these sources of systematic uncertainties:

1) Stellar mass-to-light ratio Υ_*. The uncertainty from this source can be estimated by running the fits with several values for Υ_*. For the 11 studied dwarf galaxies this uncertainty is negligible, unless Υ_* is greater than approximately $10 M_\odot/L_\odot$. For the set of 11 dwarf galaxies we set $\Upsilon_* = 1 M_\odot/L_\odot$, and ignore this uncertainty.

2) "Phase space dilution" may be an issue if the galaxy formation has relaxation,

Table 2. Presented are 11 dwarf galaxies passing the selections (see text), their reduced radial velocity dispersions $\sqrt{\langle v'^2_{rh}\rangle} \equiv \sqrt{\langle v^2_{rh}\rangle/(1-\kappa_h)}$ and $\sqrt{\langle v'^2_{rb}\rangle} \equiv \sqrt{\langle v^2_{rb}\rangle/(1-\kappa_b)}$, and their core densities $\rho_h(r_{\min})$ and $\rho_b(r_{\min})$ (calculated by integrating numerically the hydrostatic Equations (2)-(4), see text), and $v'_{hrms}(1)$ calculated with (6). The comparisons of the observed and calculated rotation curves are presented in the appendix. Uncertainties are statistical at 68% confidence. The mean and standard deviation of $v'_{hrms}(1)$ are 0.490 km/s and 0.160 km/s.

Galaxy	$\sqrt{\langle v'^2_{rb}\rangle}$ [km/s]	$\sqrt{\langle v'^2_{rh}\rangle}$ [km/s]	$\rho_b(r_{\min})$ [$10^{-3} M_\odot/\mathrm{pc}^3$]	$\rho_h(r_{\min})$ [$10^{-3} M_\odot/\mathrm{pc}^3$]	$v'_{hrms}(1)$ [km/s]
DDO 43	30.0 ± 3.2	24.2 ± 2.0	3.80 ± 0.53	21.38 ± 4.08	0.486 ± 0.072
DDO 46	78.6 ± 13.3	45.9 ± 0.9	8.49 ± 1.94	387.23 ± 39.99	0.351 ± 0.019
DDO 52	56.9 ± 5.0	38.4 ± 1.9	2.30 ± 0.24	35.80 ± 5.62	0.649 ± 0.067
DDO 87	44.0 ± 5.3	35.2 ± 1.8	0.91 ± 0.14	11.44 ± 1.45	0.871 ± 0.082
DDO 101	48.6 ± 6.5	40.7 ± 1.2	14.95 ± 4.09	366.83 ± 35.29	0.317 ± 0.019
DDO 126	25.8 ± 1.4	25.3 ± 1.4	5.48 ± 0.54	18.91 ± 2.96	0.530 ± 0.058
DDO 133	35.4 ± 1.8	28.6 ± 0.6	7.01 ± 0.62	59.32 ± 4.84	0.409 ± 0.020
DDO 154	35.6 ± 1.6	28.7 ± 0.9	3.01 ± 0.38	48.27 ± 9.96	0.440 ± 0.045
NGC 2366	40.2 ± 1.9	35.7 ± 0.9	7.69 ± 0.97	33.70 ± 4.55	0.616 ± 0.044
NGC 3738	84.4 ± 8.3	81.1 ± 2.3	105.27 ± 22.47	1823.54 ± 156.61	0.370 ± 0.021
WLM	21.7 ± 0.9	23.3 ± 0.9	10.33 ± 0.94	51.57 ± 6.49	0.349 ± 0.029

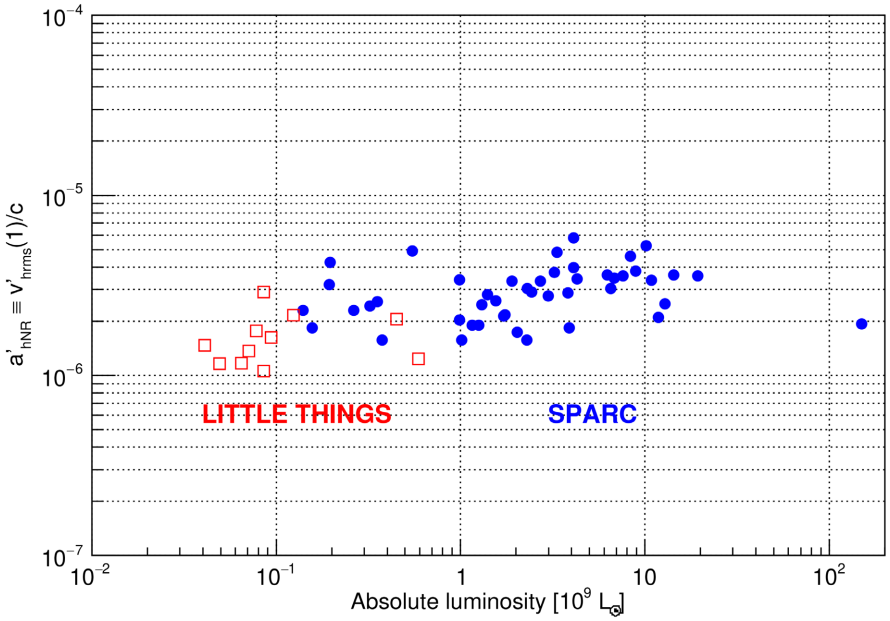

Figure 3. The expansion parameter at which dark matter becomes non-relativistic (uncorrected for dark matter rotation) $a'_{hNR} \equiv v'_{hrms}(1)/c$, as a function of the absolute luminosity, of the 11 LITTLE THINGS dwarf galaxies in **Table 2**, and the 46 spiral galaxies in the SPARC sample [5]. The absolute luminosity is in the V-band for the LITTLE THINGS sample, and 3.6 μm for the SPARC sample.

i.e. is not adiabatic. For warm dark matter, first galaxies form adiabatically [4]. In the cold dark matter scenario, galaxy formation requires relaxation and "virialization". What happens to the adiabatic invariant $v_{hrms}(1)$ when two galaxies collide, relax and merge? Does relaxation "dilute" phase space? The answer is yes and no. According to the Collisionless Boltzmann Equation, the "fine-grained" phase space density, *i.e.* the number of particles per unit phase space volume, as seen by an arbitrary particle, is constant (in the approximation that the particles are collisionless and conserved). However the "coarse-grained" phase space density can become "mixed with vaccuum", *i.e.* "diluted". Thus the coarse-grained adiabatic invariant $v_{hrms}(1)$ can increase due to relaxation (see the discussion on the coarse-grained entropy in [9], and see section 7 below).

3) Baryon disturbances due to interactions. The adiabatic invariant of a galaxy is obtained from the observed HI rotation curve $v(r)$, and the observed baryon (gas plus stars) density $\rho_b(r)$. An interaction that disturbs baryons will change the observed adiabatic invariant. From the 11 dwarf galaxies studied in this analysis, about 7 rotation curves show extraneous features, see the figures in the appendix. An extreme example is Haro 29, which appears to have had a recent interaction [15] which has distorted the measured rotation curve, see the last figure in the appendix. For Haro 29 we obtain $v'_{hrms}(1) = 0.203 \pm 0.020$ km/s (with a large χ^2 per degree of freedom), *i.e.* a fluctuation from the mean 0.490 km/s of 0.287 km/s! For these reasons we estimate that baryon perturbations are a main source of uncertainty of the measured $v_{hrms}(1)$, and may reasonably

reach an uncorrelated ± 0.1 km/s per galaxy.

4) Dark matter halo rotation. One interpretation of the width of the distributions of $v'_{hrms}(1)$ is the dark matter halo rotation correction factor $\sqrt{1-\kappa_h}$ that is different for each galaxy. If the lower edge of these distributions at $v'_{hrms}(1) \approx 0.40$ km/s correspond to $\kappa_h = 0$, then the distribution for the 11 dwarf galaxies has κ_h in the range 0 to approximately 0.8, see Figure 4, while the distribution for the 46 SPARC spiral galaxies has κ_h in the range 0 to approximately 0.95.

Note that the uncertainty of the measured $v'_{hrms}(1)$ due to relaxation and rotation is limited to the width of the distributions in Figure 2. Furthermore, both rotation and relaxation increase $v'_{hrms}(1)$, so at the lower end of the distribution of $v'_{hrms}(1)$ we should have $v'_{hrms}(1) \approx v_{hrms}(1)$. Finally, according to Table 2, rotation and relaxation only increase the adiabatic invariant by a factor at most 2.2.

Without further knowledge of the rotation and relaxation corrections, we can neglect these corrections altogether, and present, as a conservative estimate, the mean and standard deviation of the distribution in Table 2:

$$v_{hrms}(1) \approx 0.49 \pm 0.16 \text{ km/s}. \tag{10}$$

In the following sections we try to improve over this estimate.

5. Interpretation

To obtain the adiabatic invariant $v_{hrms}(1)$ we still need to obtain κ_h for each

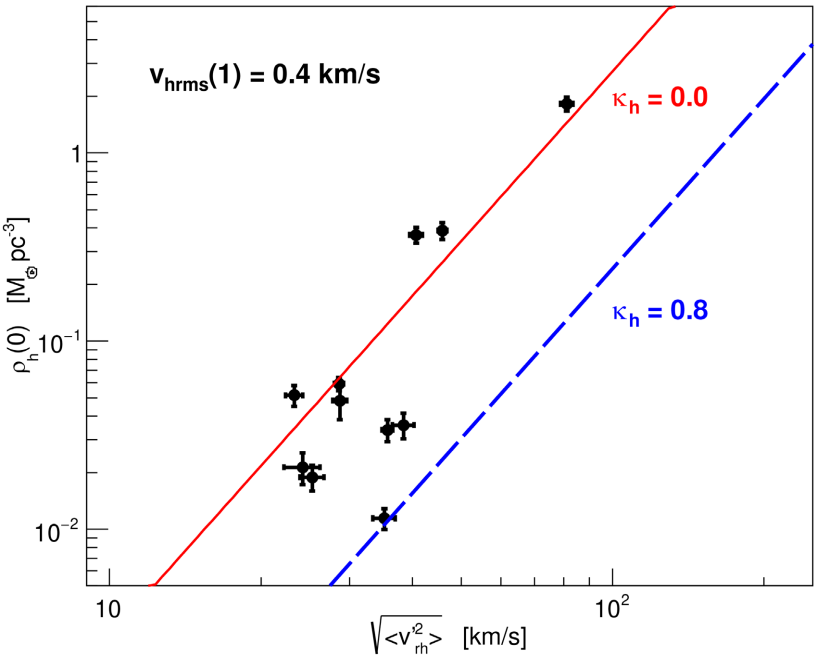

Figure 4. Shown are $\sqrt{\langle v'^2_{rh} \rangle}$ vs. $\rho_h(0)$ from Table 2, with statistical uncertainties only. The lines correspond to the adiabatic invariant $v_{hrms}(1) = 0.4$ km/s, and $\kappa_h = 0$ (red continuous line), or $\kappa_h = 0.8$ (blue dashed line).

galaxy. This rotation parameter can not be obtained from the rotation curves, so we need independent data, or assumptions, to proceed. In **Figure 4** we present $\sqrt{\langle v'^2_{rh}\rangle}$ vs. $\rho_h(0)$ for each galaxy in **Table 2**, indicating statistical uncertainties only. Superimposed on this figure we present lines corresponding to $v_{hrms}(1) = 0.4$ km/s, for $\kappa_h = 0$ and $\kappa_h = 0.8$. So, one interpretation is that galaxies near the continuous line have $\kappa_h \approx 0$, while galaxies to the right of this line have $\kappa_h > 0$ (or some other disturbance).

The distribution of $v'_{hrms}(1)$ is peaked at the low end, see **Figure 2** and **Figure 4**. We interpret this peak as corresponding to galaxies with little dark matter rotation, *i.e.* $\kappa_h \approx 0$, which are therefore likely to have experienced no major mergers. Note that a warm dark matter halo has less small scale structure than a cold dark matter halo, and so less baryon angular momentum is transferred to the warm dark matter [16]. We interpret the width of the $v'_{hrms}(1)$ peak as due to baryon disturbances, and residual dark matter halo rotation and relaxation. Since we have no reliable systematic uncertainties, we simply quote the mean and standard deviation of $v'_{hrms}(1)$ of the eight dwarf galaxies with least $v'_{hrms}(1)$ in **Table 2**, assuming they have $\kappa_h = 0$, see **Figure 4**:

$$v_{hrms}(1) = 0.406 \pm 0.069 \text{ km/s}. \tag{11}$$

The same result is obtained, from these eight dwarf galaxies in the $v'_{hrms}(1)$ peak, if we add (in quadrature), to the statistical uncertainties, an uncorrelated systematic uncertainty ± 0.19 km/s. To add the remaining three galaxies would require corrections for rotation and relaxation for these three galaxies.

Similar, complementary and/or differing viewpoints can be found in [17] [18] [19].

6. Comments

In **Table 2** we note that $\langle v'^2_{rh}\rangle \approx \langle v'^2_{rb}\rangle$, or $3\langle v'^2_{rh}\rangle \approx 2\langle v'^2_{rb}\rangle$. Is there a reason for this? Dark matter and baryons share the same gravitational potential. For a first generation galaxy we expect that $\rho_h(r)/\Omega_c$ is of order $\rho_b(r)/\Omega_b$, before baryons loose energy by radiation, see simulations in [4]. Note that the numerical solutions in [4] obtain $\rho_b(r) \propto r^{-2}$, or $\alpha \equiv \langle v'^2_{rh}\rangle / \langle v'^2_{rb}\rangle \approx 1$, before baryons loose energy by radiation. The relation $\rho_h(r) \propto \rho_b(r)$ is also approximately valid for the sample of dwarf galaxies under study, see the figures in the appendix. So, from the virial theorem applied to a sphere of radius $R \gg r_c$, separately for dark matter and baryons, we can expect that the kinetic energy per unit mass is similar for dark matter and baryons. Let K_h be the mean kinetic energy of a dark matter particle in the sphere of radius *R*. Then, twice the dark matter mean kinetic energy per unit mass, assuming equal dispersions in the 3 dimensions, is

$$2\frac{K_h}{m_h} = 3\langle v^2_{rh}\rangle + \kappa_h v^2 = 3\langle v^2_{rh}\rangle + \kappa_h 2\frac{\langle v^2_{rh}\rangle}{1-\kappa_h} = (3-\kappa_h)\langle v'^2_{rh}\rangle. \tag{12}$$

A similar equation holds for baryons. If dark matter and baryon particles are mainly supported by rotation, *i.e.* if κ_h and κ_b are approximately 0.99, then

$\langle v'^2_{rh}\rangle \approx \langle v'^2_{rb}\rangle$. If dark matter is supported mainly by dispersion, *i.e.* $\kappa_h \approx 0$, while baryons are supported mainly by rotation, then $3\langle v'^2_{rh}\rangle \approx 2\langle v'^2_{rb}\rangle$. In conclusion, the approximate equality of $\langle v'^2_{rh}\rangle$ and $\langle v'^2_{rb}\rangle$ can be understood.

The observed baryon 1-dimensional velocity dispersion, in the sample of 11 dwarf galaxies, e.g. DDO 43, is $\sqrt{\langle v^2_{rb}\rangle} \approx 4$ km/s [6]. For $\sqrt{\langle v'^2_{rb}\rangle} \approx 30$ km/s, we obtain $\kappa_b \approx 0.98$. If $\langle v^2_{rh}\rangle \ll \langle v^2_{rb}\rangle$, then $1-\kappa_h \ll 1-\kappa_b$, so $\kappa_h \approx 1$, and dark matter particles rotate on very nearly circular orbits. If $\langle v^2_{rh}\rangle \gg \langle v^2_{rb}\rangle$, then $1-\kappa_h \gg 1-\kappa_b$, so $\kappa_b \approx 1$, and baryons rotate on nearly circular orbits, in a plane due to collisions, as observed. In the warm dark matter scenario, velocities in first generation galaxies are nearly isotropic in the core, and increasingly radial at larger r (from the simulations in [4]), while collisions and mergers may change this.

7. Relaxation

The following thought toy experiments have helped me try to understand relaxation. Consider warm dark matter in a box. The dark matter particles are collisionless, except with the walls of the box (that represent gravity). Now put two boxes side-by-side, one full and one empty of dark matter, and remove the dividing wall. Particle velocities are unchanged. The particle density is halved, so the "coarse-grained" adiabatic invariant has increased by a factor $2^{1/3}$. If velocities are reversed *exactly*, the dark matter particles return to their original box, so the "fine-grained" adiabatic invariant has remained unchanged.

Now consider two full boxes that collide. At the moment of the collision the boxes are stopped, and the dividing wall is removed. The dark matter density is unchanged. The dark matter particle velocities are unchanged. However, the velocity dispersion with respect to the center-of-mass has increased, so the "coarse-grained" adiabatic invariant has increased. If the collision is offset, the dark matter acquires angular momentum, which again increases the observed $v'_{h\mathrm{rms}}(1)$.

We can now understand the three galaxies farthest to the right of the continuous red line in **Figure 4**: these galaxies have undergone one or more major interactions and mergers, and so have acquired angular momentum and/or relaxation, resulting in an increase of $v'_{h\mathrm{rms}}(1)$. On the other hand, the eight galaxies near the continuous red line are pristine (in our interpretation), they have little rotation, *i.e.* $\kappa_h \approx 0$, and have not encountered major interactions. These pristine dwarf galaxies should contain a few first or second generation stars with little or no metallicity.

8. Conclusions

The results summarized in **Table 2** are obtained directly from the rotation curves in reference [6] of 11 dwarf galaxies dominated by dark matter, see the excellent fits in the appendix. The distribution of $v'_{h\mathrm{rms}}(1)$ in **Table 2** and **Figure 2** has a mean 0.49 km/s, a standard deviation 0.16 km/s, and is peaked at low

$v'_{hrms}(1)$. We apply a mild, data driven, rotation and relaxation correction that obtains the adiabatic invariant in the core of the galaxies:

$$v_{hrms}(1) = 0.406 \pm 0.069 \text{ km/s}. \quad (13)$$

These two small relative standard deviations justify the prediction that the adiabatic invariant $v_{hrms}(1)$ in the core of the galaxies is of cosmological origin if dark matter is warm. This result is in agreement with independent measurements of $v_{hrms}(1)$, summarized in Table 3 of [20], based on spiral galaxy rotation curves, galaxy rest frame ultra-violet luminosity distributions, galaxy stellar mass distributions, the formation of first galaxies, reionization, and the velocity dispersion cut-off mass.

Conflicts of Interest

The author declares no conflicts of interest regarding the publication of this paper.

References

[1] Paduroiu, S., Revaz, Y. and Pfenniger, D. (2015) Structure Formation in Warm Dark Matter Cosmologies Top-Bottom Upside-Down.. https://arxiv.org/pdf/1506.03789.pdf

[2] Hoeneisen, B. (2022) Comments on Warm Dark Matter Measurements and Limits. *International Journal of Astronomy and Astrophysics*, **12**, 94-109. https://doi.org/10.4236/ijaa.2022.121006

[3] Particle Data Group, Workman, R.L. *et al.* (2022) Review of Particle Physics. *Progress of Theoretical and Experimental Physics*, **2022**, 083C01. https://doi.org/10.1093/ptep/ptac097

[4] Hoeneisen, B. (2022) Warm Dark Matter and the Formation of First Galaxies. *Journal of Modern Physics*, **13**, 932-948. https://doi.org/10.4236/jmp.2022.136053

[5] Hoeneisen, B. (2019) The Adiabatic Invariant of Dark Matter in Spiral Galaxies. *International Journal of Astronomy and Astrophysics*, **9**, 355-367.

[6] Oh, S., *et al.* (2015) High-Resolution Mass Models of Dwarf Galaxies from LITTLE THINGS. *The Astronomical Journal*, **149**, 180. https://doi.org/10.1088/0004-6256/149/6/180

[7] Mo, H., van den Bosch, F. and White, S. (2010) Galaxy Formation and Evolution. Cambridge University Press, Cambridge.

[8] Hoeneisen, B. (2019) A Study of Dark Matter with Spiral Galaxy Rotation Curves. *International Journal of Astronomy and Astrophysics*, **9**, 71-96. https://doi.org/10.4236/ijaa.2019.92007

[9] Binney, J. and Tremaine, S. (2008) Galactic Dynamics. 2nd Edition, Princeton University Press, Princeton. https://doi.org/10.1515/9781400828722

[10] Hoeneisen, B. (2021) A Study of Three Galaxy Types, Galaxy Formation, and Warm Dark Matter. *International Journal of Astronomy and Astrophysics*, **11**, 489-508. https://doi.org/10.4236/ijaa.2021.114026

[11] Kormendy, J. and Freeman, K.C. (2015) Scaling Laws for Dark Matter Halos in Late-Type and Dwarf Spheroidal Galaxies. *The Astrophysical Journal*, **817**, 84. https://doi.org/10.3847/0004-637X/817/2/84

[12] Hunter, D.A., Ficut-Vicas, D., Ashley, T., *et al.* (2012) LITTLE THINGS. *The Astronomical Journal*, **144**, 134. https://doi.org/10.1088/0004-6256/144/5/134

[13] Kennicutt Jr., R.C., Armus, L., Bendo, G., *et al.* (2003) SINGS: The SIRTF Nearby Galaxies Survey. *Publications of the Astronomical Society of the Pacific*, **115**, 928. https://doi.org/10.1086/376941

[14] Hunter, D.A. and Elmegreen, B.G. (2006) Broadband Imaging of a Large Sample of Irregular Galaxies. *The Astrophysical Journal Supplement Series*, **162**, 49-79. https://doi.org/10.1086/498096

[15] Ashley, T., Simpson, C.E. and Elmegreen, B.G. (2013) The HI Chronicles of LITTLE THINGS BCDs: Evidence for External Perturbations in the Morphology and Kinematics of Haro 29 and Haro 36. *The Astronomical Journal*, **146**, Article No. 42. https://doi.org/10.1088/0004-6256/146/2/42

[16] Sommer-Larsen, J. and Dolgov, A. (2001) Formation of Disk Galaxies: Warm Dark Matter and the Angular Momentum Problem. *The Astrophysical Journal*, **551**, 608-623. https://doi.org/10.1086/320211

[17] Hogan, C.J. and Dalcanton, J.J. (2000) New Dark Matter Physics: Clues from Halo Structure. *Physical Review D*, **62**, Article ID: 063511. https://doi.org/10.1103/PhysRevD.62.063511

[18] Dalcanton, J.J. and Hogan, C.J. (2001) Halo Cores and Phase-Space Densities: Observational Constraints on Dark Matter Physics and Structure Formation. *The Astrophysical Journal*, **561**, 35. https://doi.org/10.1086/323207

[19] Karukes, E.V. and Salucci, P. (2016) The Universal Rotation Curve of Dwarf Disc Galaxies. *Monthly Notices of the Royal Astronomical Society*, **465**, 4703-4722. https://doi.org/10.1093/mnras/stw3055

[20] Hoeneisen, B. (2022) Measurement of the Dark Matter Velocity Dispersion with Galaxy Stellar Masses, UV Luminosities, and Reionization. *International Journal of Astronomy and Astrophysics*, **12**, 258-272. https://doi.org/10.4236/ijaa.2022.123015

Appendix. Circular Velocities and Densities

The figures below present the circular velocities $v(r)$, and densities of dark matter $\rho_h(r)$ and baryons (gas plus stars) $\rho_b(r)$, and their sum $\rho_{\text{tot}}(r) = \rho_h(r) + \rho_b(r)$, as a function of the distance r from the center of each galaxy. $v(r)$ is the velocity of a test particle in a circular orbit of radius r in the plane of the baryon disk, and has contributions from dark matter and baryons: $v(r) = \sqrt{v_h^2(r) + v_b^2(r)}$. The data points are obtained from [6]. The continuous lines are obtained by numerical integration of the hydrostatic equations (2), (3) and (4), that require four boundary conditions to start the integration [8]: $\sqrt{\langle v'^2_{rb} \rangle}$, $\sqrt{\langle v'^2_{rh} \rangle}$, $\rho_b(r_{\min})$, and $\rho_h(r_{\min})$, where $r_{\min}$ is the smallest measured r. These four parameters are varied to minimize a χ^2 between the data and the numerical integration. The results are presented in Table 2. The indicated uncertainties of $v_b(r)$ are estimated from their fluctuations.

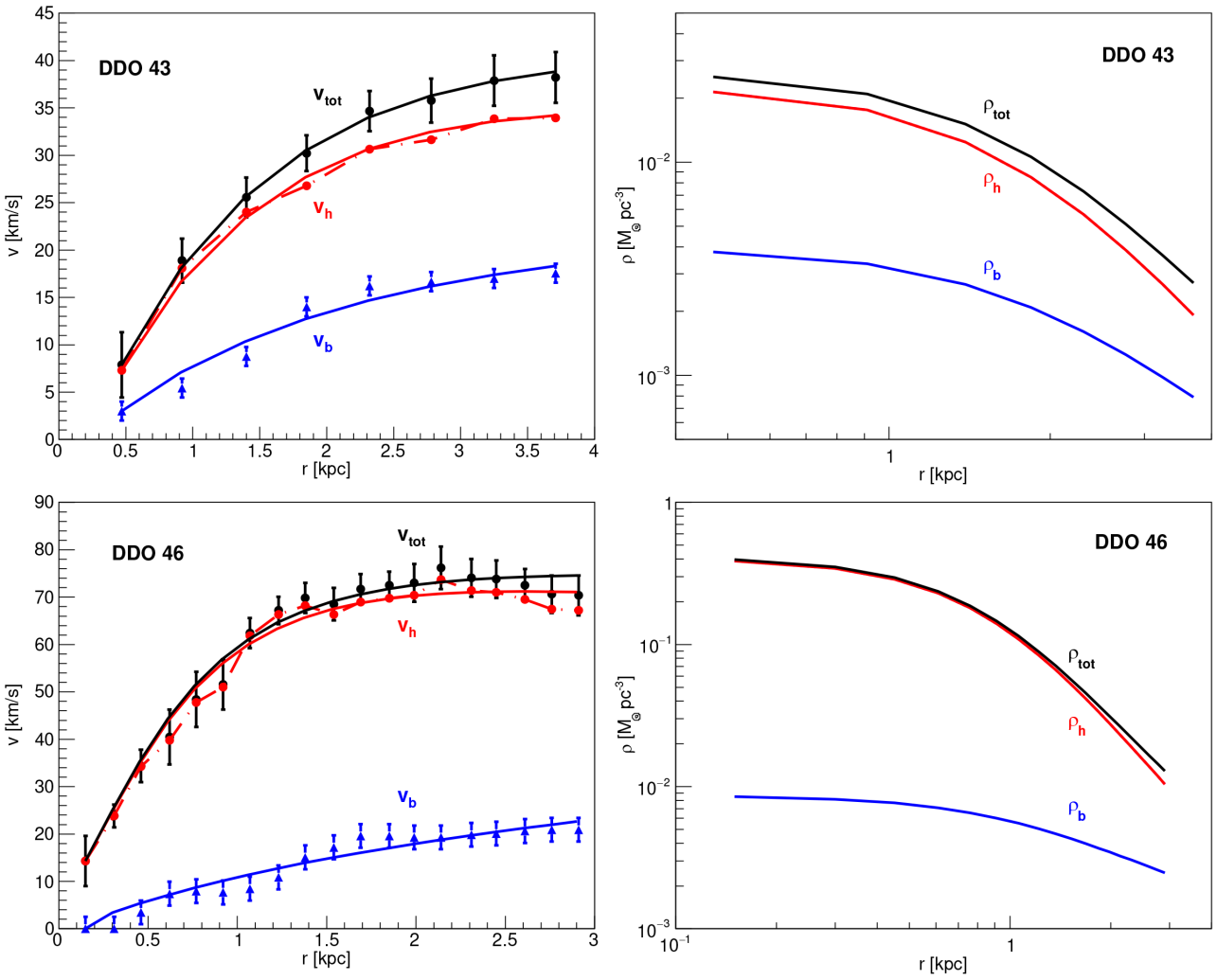

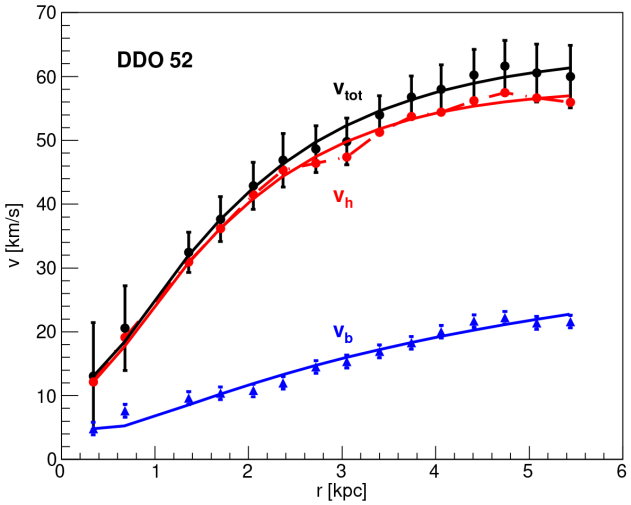
DDO 52
v_{tot}
v_h
v_b
v [km/s]
r [kpc]

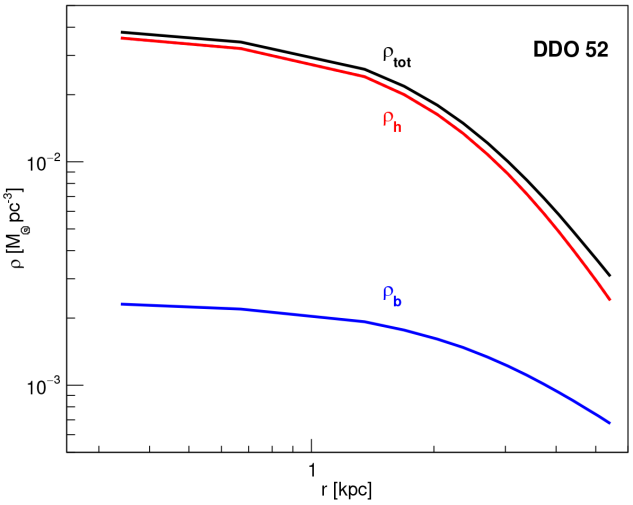
DDO 52
ρ_{tot}
ρ_h
ρ_b
ρ [$M_\odot$ pc^{-3}]
r [kpc]

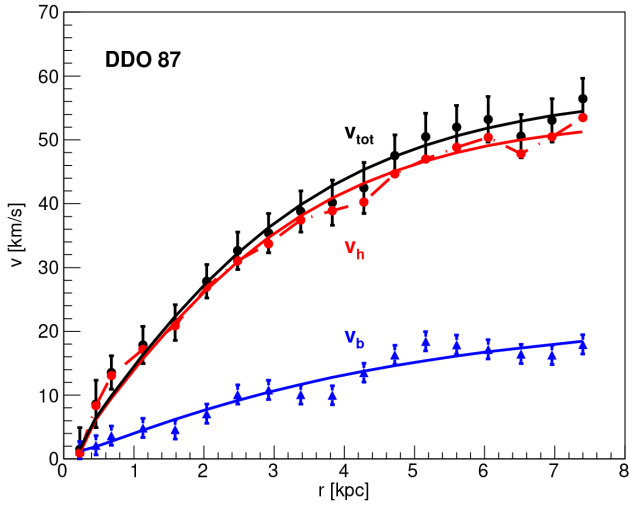
DDO 87
v_{tot}
v_h
v_b
v [km/s]
r [kpc]

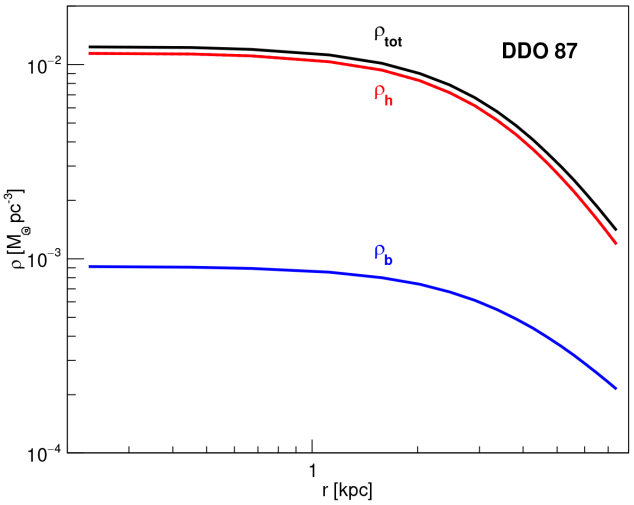
DDO 87
ρ_{tot}
ρ_h
ρ_b
ρ [$M_\odot$ pc^{-3}]
r [kpc]

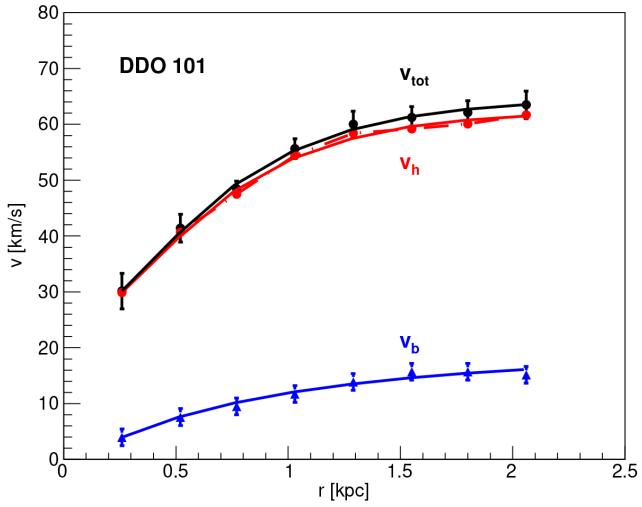
DDO 101
v_{tot}
v_h
v_b
v [km/s]
r [kpc]

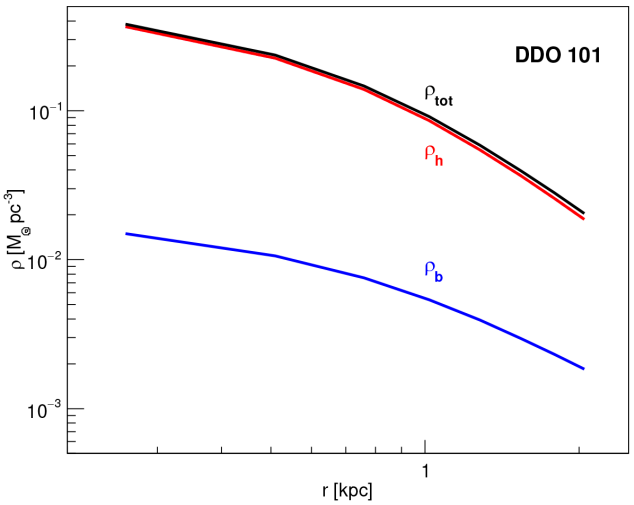
DDO 101
ρ_{tot}
ρ_h
ρ_b
ρ [$M_\odot$ pc^{-3}]
r [kpc]

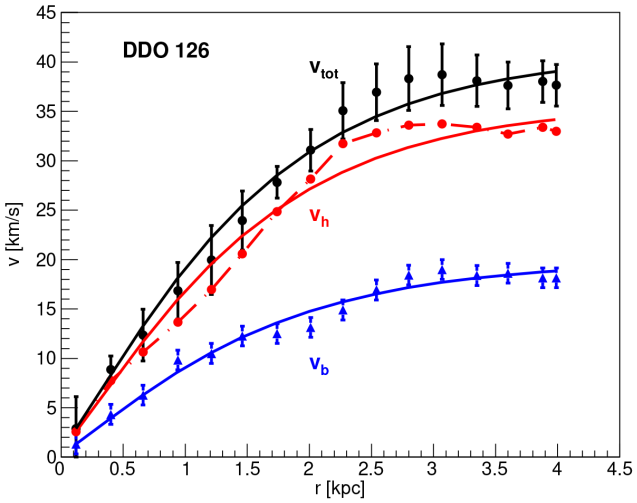
DDO 126
v_{tot}
v_h
v_b
v [km/s]
r [kpc]

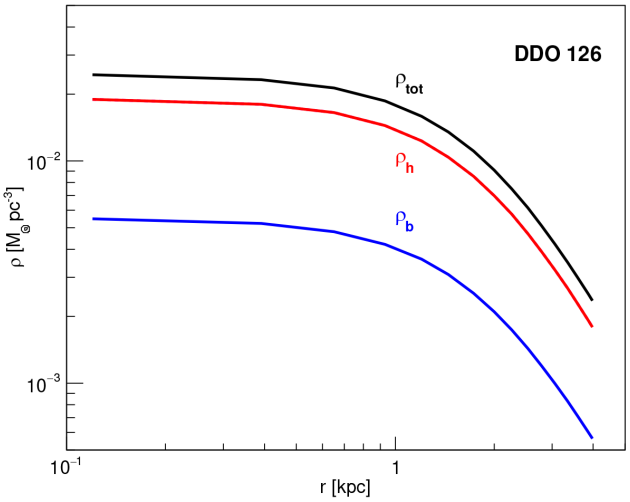
DDO 126
ρ_{tot}
ρ_h
ρ_b
ρ [$M_\odot$ pc^{-3}]
r [kpc]

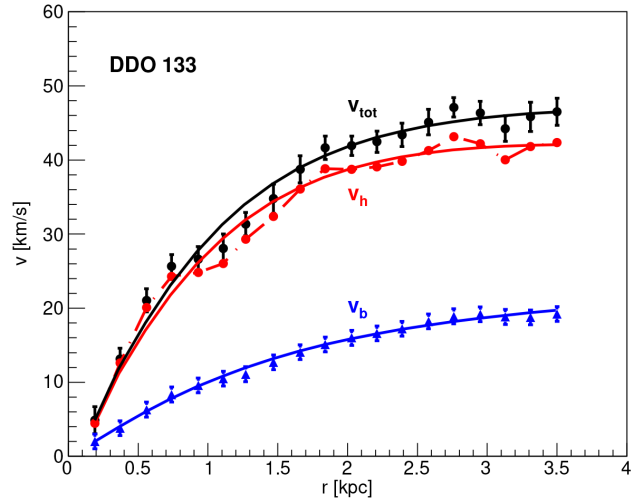
DDO 133
v_{tot}
v_h
v_b
v [km/s]
r [kpc]

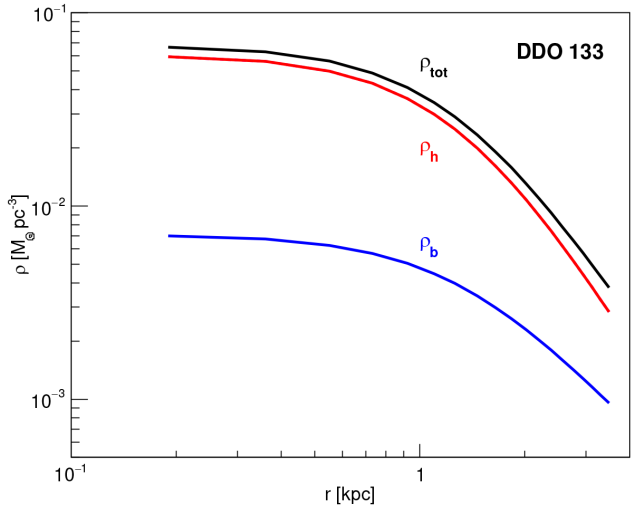
DDO 133
ρ_{tot}
ρ_h
ρ_b
ρ [$M_\odot$ pc^{-3}]
r [kpc]

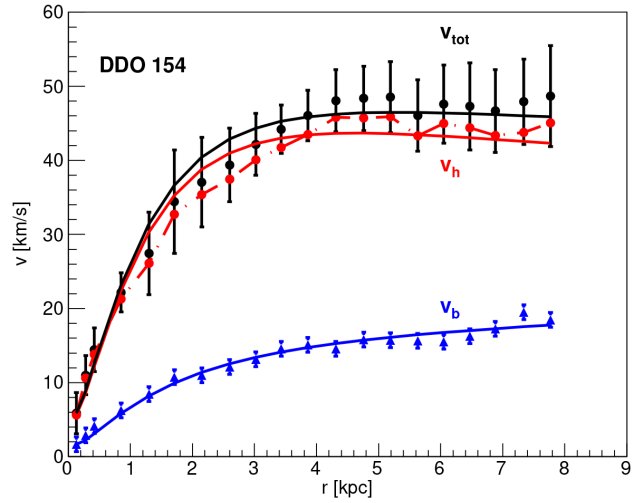
DDO 154
v_{tot}
v_h
v_b
v [km/s]
r [kpc]

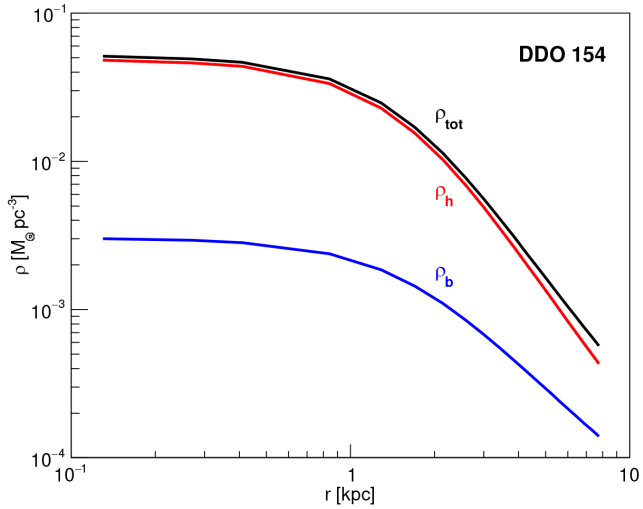
DDO 154
ρ_{tot}
ρ_h
ρ_b
ρ [$M_\odot$ pc^{-3}]
r [kpc]

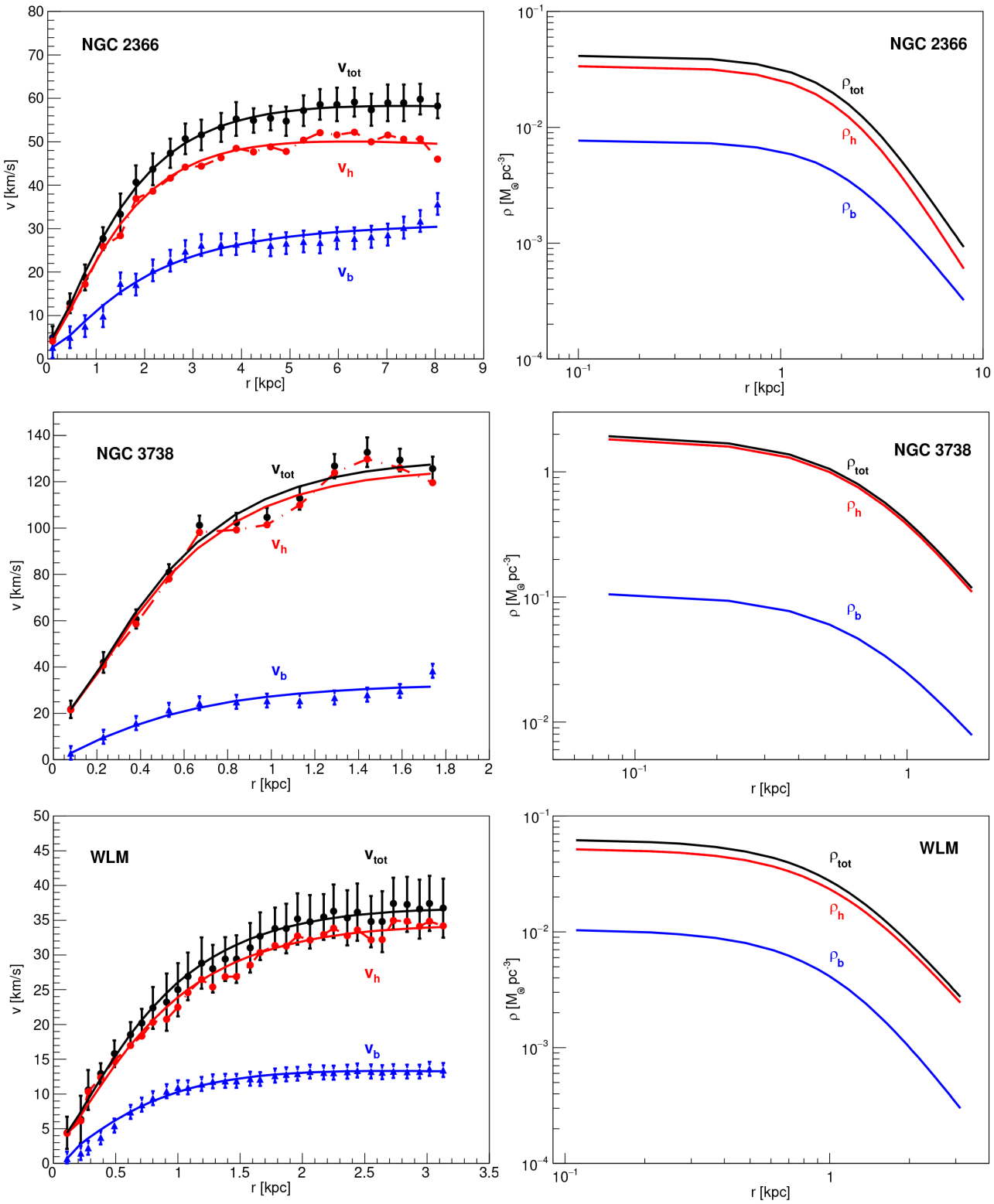
NGC 2366
v_tot
v_h
v_b
v [km/s]
r [kpc]
NGC 2366
ρ_tot
ρ_h
ρ_b
ρ [M_⊙ pc^-3]
r [kpc]
NGC 3738
v_tot
v_h
v_b
v [km/s]
r [kpc]
NGC 3738
ρ_tot
ρ_h
ρ_b
ρ [M_⊙ pc^-3]
r [kpc]
WLM
v_tot
v_h
v_b
v [km/s]
r [kpc]
WLM
ρ_tot
ρ_h
ρ_b
ρ [M_⊙ pc^-3]
r [kpc]

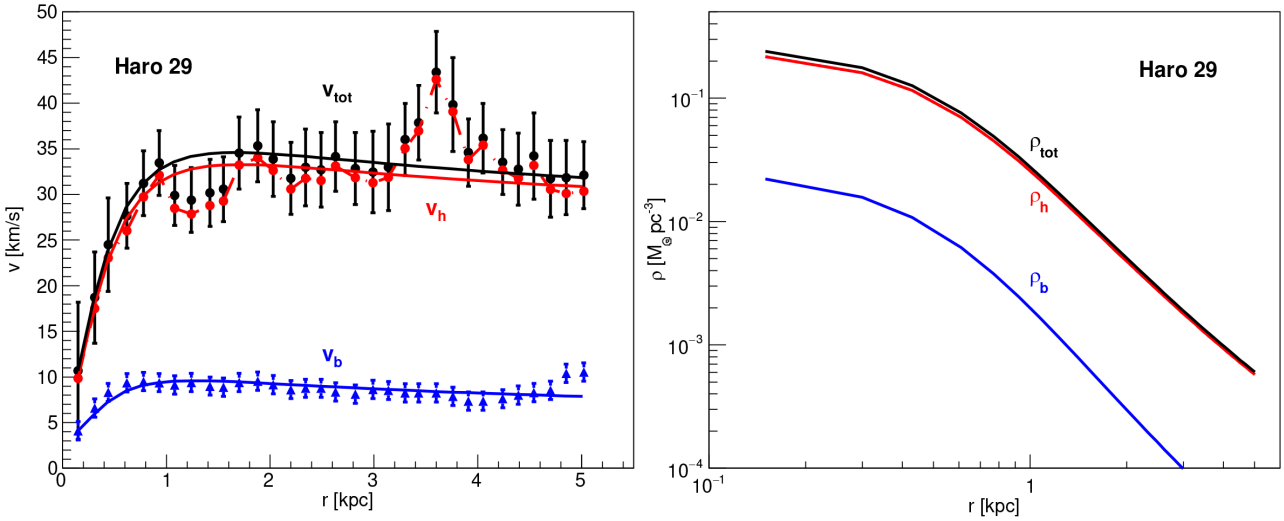
Haro 29
v_{tot}
v_h
v_b
v [km/s]
r [kpc]
Haro 29
ρ_{tot}
ρ_h
ρ_b
ρ [$M_\odot$ pc^{-3}]
r [kpc]